Studies on Erosion of Atmospheric Plasma Sprayed NiCrBSi/Mo/Flyash Coating

Nagabhushana N
Senior Assistant Professor,
New Horizon College of Engineering,
Bangalore-560103, India

Dr. M.R Ramesh
Associate Professor,
National Institute of Technology,
Suratkal-575014, India

Dr. Rajanna S
Associate professor,
Government Engineering College,
Kushalnagar-571234, India

Padmini B.V
Assistant Professor,
Sambhram Institute of Technology,
Bangalore-560097, India

***Abstract* - In the current work, the erosion behavior of plasma sprayed NiCrBSi/Mo/Flyash cenosphere coating deposited on Super Ni76 steel was studied. The coating was characterized using a scanning electron microscope (SEM). Microhardness, porosity, fracture toughness and ductility of the coating were quantified. The solid particle erosion test was carried out at room temperature using alumina powder at 30° and 90° impact angles. The erosion resistance of the coating was observed to be higher at lower impact angles. The stability of the molybdenum, alumina and oxide layers helps to improve the corrosion resistance of the coating. The eroded coating surface morphology reveals a brittle pattern of material removal.**

Key words: Substrate, Coating, Erosion, Plasma spray

1. INTRODUCTION

Aircraft engines operating in sandy environments are severely damaged by sand on compressor blades, vanes, or impeller blades/wheels. Damage may occur on these components due to the pitting and cut of the leading edge, the trailing edge becoming thinner and the blade chord length shortening. Physical changes in blade geometry due to erosion affect the dynamic response characteristics of the compressor airfoil, and the column results in increased fuel consumption and reduced life of the hot portion of the engine. A large amount of material removal not only leads to further aerodynamic losses, but also leads to weakening of the structure of the blade. When the damage is too large, component integrity and aircraft safety are affected. Due to excessive corrosion of the compressor blades, some helicopters were removed from the site early. Replacing parts with corrosion damage limitations has been costly and can lead to logistical problems with engine availability. There are several ways to minimize corrosion damage in gas turbine engines, including the use of air intake filtration, improved engine design, optimized intake positioning, and the application of corrosion resistant coatings on component surfaces. Integral transition metal nitride coatings such as TiN, CrN, TiAlN and TiSiN have been investigated as corrosion resistant coatings for engine components. TiN coatings were first implemented by Russia during its military involvement in Afghanistan, where sand erosion severely limited the life of helicopter turbine engines. Although it provides excellent protection against erosion of the compressor blades at low sand impact angles, it is susceptible to cracking and spalling from the substrate due to its brittleness, particularly when impacted by high velocity particles at high angles. A CrN coating having a higher toughness than TiN is disadvantageous as a candidate for corrosion resistance applications because it is insufficient to effectively resist particle removal materials by micro-cutting. In general, coatings with high hardness and toughness can withstand impact loads and resist crack formation, resulting in excellent resistance to solid particle erosion. Although monolithic binary transition metal nitrides are often difficult to achieve such a combination of mechanical properties, they can be achieved by introducing alloying elements, changing the microstructure and structure of the coating, or using a combination of the two. Coatings with a multilayer structure may be harder and tougher than a uniform coating of the same material because the layered structure hinders dislocation slip and crack propagation. The toughening of the multilayer structure is attributed to the effect of the interface on the dissipation of fracture energy and deflection cracks. The nano-layered coating consists of nano-scale multilayer alternating materials with a modulation period between a few nanometers and a few hundred nanometers. It is also expected to achieve high hardness and toughness due to interface toughening. Therefore, it has been reported that the improved erosion performance of some nanolayer and multilayer coating systems is not surprising.

Erosion is a phenomenon of material removal caused by solid particles hitting a target surface. Solving corrosion of components operating at high temperatures becomes negligible and complex, as in gas and steam turbines, jet engine components, coal-fired power plant boiler tubes, and the like. The nickel and stainless steel alloys used in these components provide good mechanical strength. However, they lack better erosion, wear and corrosion resistance, resulting in a shorter service life. The corrosion resistance of these components can be enhanced by suitable surface modification

techniques such as thermal spray coating. Among the available thermal spray coatings, plasma spray is widely used in wear resistant applications. Using available MCrAlY coatings, NiCrAlY is widely used in oxidation, corrosion and wear applications. However, these coatings have industrial limitations due to lower hardness compared to carbides, ceramics and oxides. However, by strengthening WC, Al2O3, Cr3C2, Cr2O3, TiC, TiO, SiC, TiN, CeO2, ZrO2 and other hard phases, the corrosion resistance of these coatings can be significantly improved. WC-Co has higher hardness and good ductility, chemical inertness, lower friction coefficient than Cr3C2. These properties improve the wear resistance of the WC-Co coating and may enhance the corrosion resistance of NiCrAlY. However, NiCrAlY and WC-Co powders are expensive, limiting the wide adaptability to various structural components. The use of industrial waste such as fly ash cenosphere microbeads, which can be obtained in large quantities and inexpensive, can be a desirable constituent material in such coatings.

Fly ash is a by-product of combustion of coal in thermal power plants. They are spherical, inexpensive, easy to obtain in powder form and have excellent mechanical properties. Fly ash is mainly composed of oxides of silicon (SiO2), aluminum (Al2O3), iron (Fe2O3) and mullite (3Al2O3.2SiO2). Among them, alumina and mullite have high temperature stability, wear resistance and corrosion resistance. These properties are well utilized if fly ash is used in the coating. Some researchers have studied the feasibility of fly ash as a coating material. Mishra et al. The suitability of fly ash as a raw material was investigated using a plasma spray method. Rama Krishna and others. The hardness and sliding wear behavior of fly ash coating deposited by detonation spraying technique on low carbon steel were studied. They report that fly ash coatings have better hardness and coefficient of friction than low carbon steels. Sidhu et al. Estimate the wear, oxidation and salt corrosion behavior of plasma sprayed fly ash coatings. Their research shows that fly ash coatings have better resistance to oxidation and salt corrosion than carbon steel substrates. Sahu et al. proposed the effect of plasma torch power level on the erosion behavior of pre-blended aluminum plasma sprayed fly ash. It has been reported in their research that the addition of aluminum increases the corrosion resistance of the coating. Behera and Mishra studied a plasma sprayed fly ash composite coating of quartz and ilmenite mixed on a copper substrate. The results show that the interface between the substrate and the coating is better. Recently, there have been few studies on composite coatings of fly ash. However, they lack the high temperature erosion response of the fly ash coating. This fact requires the high temperature erosion behavior of the NiCrBSi-20Mo-20 fly ash cenosphere coating proposed by the Institute. The use of these environmental contaminants in coatings may further reduce the landfill burden and is environmentally friendly if successfully developed.

Thermal spray systems have been widely used in a variety of industries, including energy conversion and utilization systems, to apply metal coatings to prevent high temperature corrosion or surface degradation caused by combined corrosion. Various types of coated alloys, such as Ni, Fe and Co bases, are widely used in corrosive environments such as boilers and turbines. Some iron-based and cobalt-based coatings have been accepted by boiler equipment as a preferred erosion protection in heat exchanger tubes in coal fired boilers. Many researchers have studied the erosion of nickel-based alloy coatings. Mishra et al. Impact and impact angles of 30^0 and 90^0 were investigated at a speed of 40 m/s, and the Ni-20Cr coating was reported to exhibit the highest erosion rate at two impact angles. The solid particle erosion behavior of NiCr and Stellite-6 coatings was evaluated using an air jet corrosion tester. It has been reported that NiCr coatings perform better than Stellite-6 coatings during solid particle erosion at 30^0 and 90^0 impact angles. Hejwowski et al. The corrosion wear behavior of the flame sprayed NiCrSiB coating was studied and it was found that NiCrSiB has better wear resistance than steel. Stein et al. Solid particle erosion of cermet (FeCrAlY-CrC and NiCr-CrC) coatings was investigated and erosion testing was performed using particle accelerator devices set at speeds of 40 m/s and 400°C and Al2O3 particles at 30^0 and 90^0 impact angles. The erosion rate of the 90^0 impact angle was found to decrease, while for the 30^0 impact angle, the erosion rate remained fairly constant.

Erosion is one of the types of wear, accounting for about 8% of all wear characteristics. Erosion is a very complicated phenomenon. Through systematic analysis, a large number of experimental and theoretical analyses have been carried out mainly on the effects of wear mechanisms and wear parameters, including corrosion, targets (erosion materials), corrosion process parameters and some environmental media. There are many factors that play a role in the corrosion resistance of the target, such as hardness, toughness, thermal conductivity, modulus of elasticity, and the like. There are two equations:

$$1/W = \alpha \cdot K^2_{Ic} \cdot H^{3/2} \quad \text{(Eq 1)}$$

$$1/W = \alpha \cdot K^{3/4}{}_{Ic} \cdot H^{1/2} \quad \text{(Eq 2)}$$

where, 1/W is erosion resistance (W is the mass loss of the target) and K_{Ic} and H are fracture toughness and hardness of the target, respectively. These two equations imply that the wear resistance of the target is proportional to $K^{\alpha}_{Ic} \cdot H^{\beta}$ ($\alpha, \beta > 0$).

In this study, a NiCrBSi-20Mo-20Fly ash coating was deposited on a Super Ni76 steel substrate using an atmospheric plasma spray process. In addition, the sample was characterized by microstructure. The erosion behavior of the coating and substrate was investigated at room temperature using Al2O3 erosion with an impact angle of 30° and 90°. The weight loss and volume loss methods are used to estimate erosion losses. The erosion mechanism was discussed using SEM and EDS.

2. MATERIALS AND METHODS

2.1. Materials

Super Ni76 steel purchased from Mishra Dhatu Nigam Ltd. of Hyderabad, India was used as a substrate. Table 1 lists the chemical composition of the Super Ni76 steel substrate. The substrate was cut to a size of 25 x 20 x 3 mm prior to plasma

spraying. Commercially available gas atomized NiCrBSi, agglomerated and sintered Mo powder and fly ash hollow microbeads are used as coating materials. The nominal particle size distribution of the powder was measured by laser diffraction technique (Cilas 1064, France).

Table 1: Chemical composition (wt %) for various steels

Type of substrate	ASTM code	Composition	C	Mn	Si	S	P	Cr	Mo	Fe	C0	W	B	Ti	Ni
Super Ni 76	Hastelloy X	Nominal	0.08	-	2	-	-	18	-	Bal	-	-	-	0.4	11.5
		Actual	0.10	1.46	0.55	0.005	0.013	18.13	-	Bal	-	-	-	0.62	10.36

These powders were mechanically mixed with a mass fraction of NiCrBSi-20Mo and 20% Flyash/hollow microbeads prior to spraying. Figure 2 shows a photomicrograph as a mixture of mixed powders. The uniform dispersion of the hollow microspheres in the NiCrBSi-20Mo-20Flyash network is evident in the applicability and feasibility of the mechanical mixing used in the microscopy.

2.2. Coating deposition

A NiCrBSi-20Mo-20Flyash hollow microbead mixture was deposited by atmospheric pressure plasma spraying using a METCO USA 3MB apparatus (M/s. Aum Technospray Pvt. Ltd., Bangalore, India). Prior to spraying, the substrate was sandblasted with 150 µm sized alumina powder to promote better adhesion between the coating and the substrate. The details of the spray parameters are listed in Table 2. During plasma spraying, the powder supplied through the feeder is mixed with argon gas flowing from the compressor at a selected pressure. The mixture flows to the plasma stream and deposits on the substrate. The deposition of each pass of the coating is in the range of 12-15 µm with a spray efficiency of 40-45% because the surface of the sprayed coating is as shown in fig. The thickness of the developed coating was quantified by SEM. The porosity of the coating was calculated using an optical microscope supported by a Biovis image analyzer (ARTRAY, AT 130, JAPAN). 20 fields of view were analyzed and the average was reported.

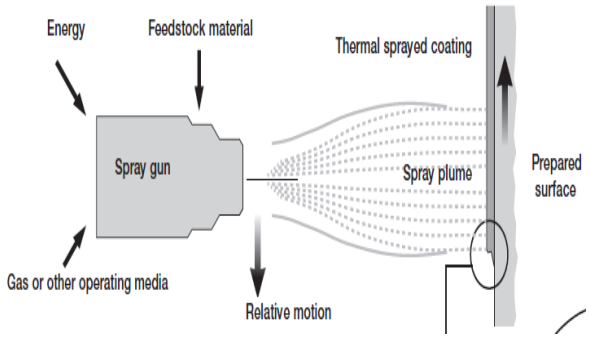

Fig 1 Plasma spray process

Argon	Pressure	100-120 psi
	Flow	150-165 lpm
Hydrogen	Pressure	50 psi
	Flow	5-7 lpm
Current		1350 amps
Voltage		60-70V
Powder feed		120-150 gm/min
Stand of Distance		4-5 inches

Table 2: Plasma Spray process parameters

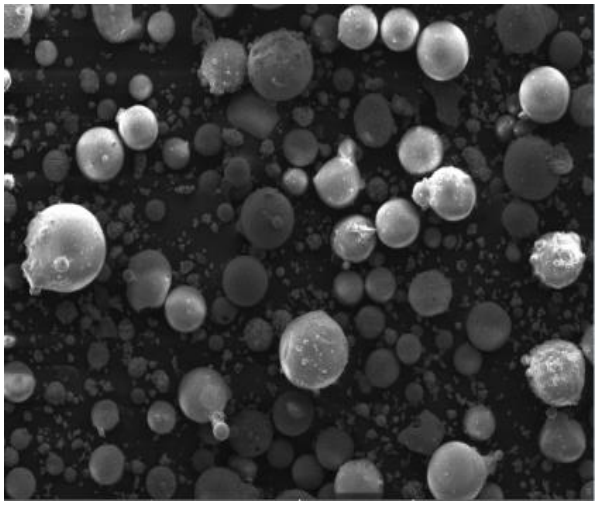

Fig.2 Powder particles

Fig.3 As-sprayed surface

2.4. Ductility

The load-displacement data obtained from the nano indentation test was used to calculate the coating ductility. The ductility is the ratio of plastic work, Wp to total work, Wt. Wp is obtained from the area enclosed by the loading and unloading curves, where the area under the loading curve is represented by Wt in the load-displacement diagram. A nano indentation test (Agilent, G200, USA) performed a 30g load on the polished surface of the coating, which was selected based on the coating thickness. The surface of the coating was polished down to 1000 grits of emery paper. Nano indentation was performed at 10 different locations and the average value is reported.

2.5. Erosion study

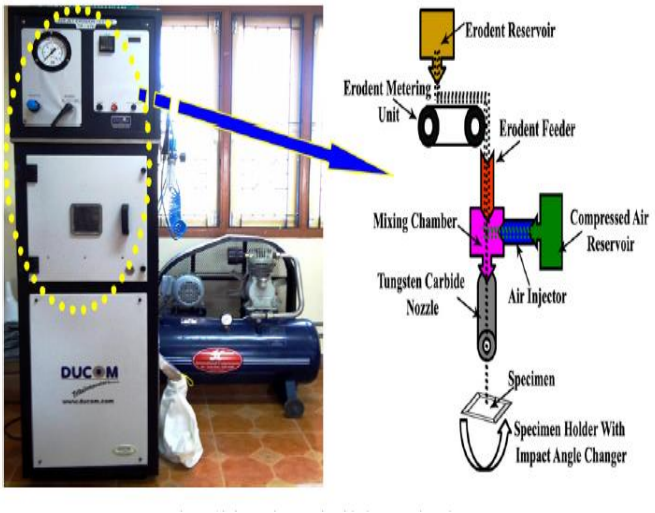

Fig.4a Schematic representation of the erosion setup

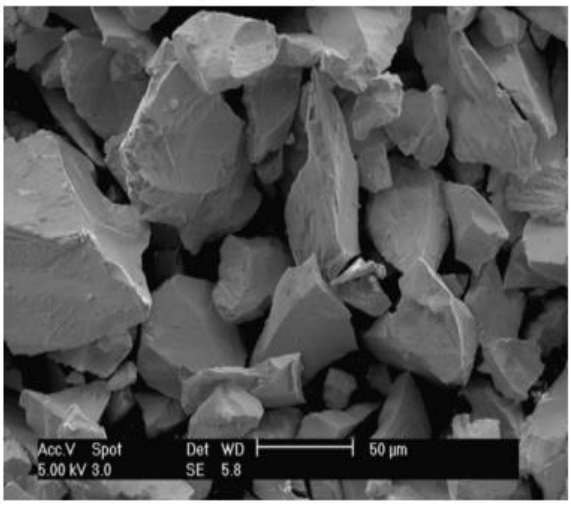

Fig.4b Sharp edged Al_2O_3 particles used for erosion testing

Solid particle erosion testing was performed according to ASTM G76-13 using an air jet erosion tester (TR-471-800, Ducom instruments Pvt. Ltd., Bangalore, INDIA). Alumina sand (Fig. 4b) is used as an etchant. A schematic of the test device is shown in Figure 4a. The Erodent and air mixture was fed into the mixing chamber at a rate of 2 g/min, which was mixed with air flowing through a tube. This erodent and air mixture impacted the sample at a rate of 30 m/s, which was rigidly fixed in the sample holder. The erosion rate was measured by the double disk method before the test. The impact angle is set by changing the direction of the sample holder relative to the erodent flow. Prior to the erosion test, the samples were cleaned in acetone, dried and sandwiched in an erosion device. After each test, the samples were washed in acetone, dried and weighed using an electronic weighing balance (minimum count 0.0001 g) to estimate mass loss. The erosion rate is calculated by the ratio of mass loss to erodent particle mass.

3. RESULTS AND DISCUSSION

3.1 Microstructure analysis of coating:

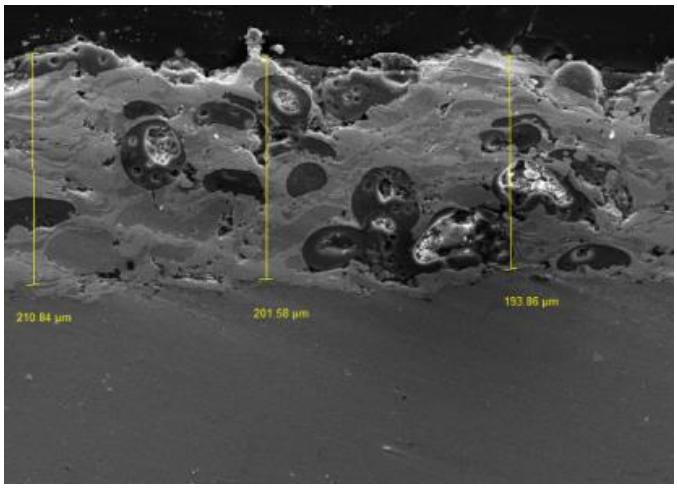

Fig.5a Coating thickness across section

An SEM micrograph of the cross section of the coating is shown in Figure 5a. As can be seen from the photomicrograph, the coating adhered well to the substrate and showed uniform dispersion of the cenospheres. The average thickness of the coating observed was 205 µm and the average area porosity was 4 ± 0.3%. Figure 5b depicts the elemental mapping of the coating, which clearly shows the different splats enriched in oxygen, coexisting with aluminum, silicon and iron, indicating the presence of the corresponding oxide.

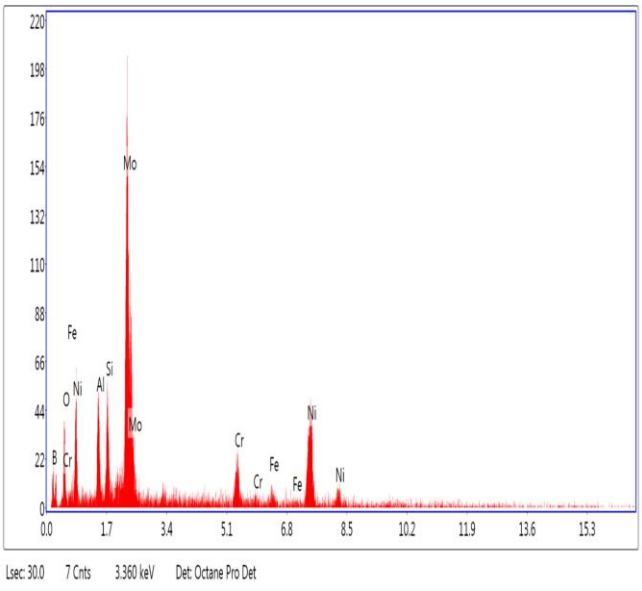

Fig.5b Elemental mapping of the coating

3.1 Response Surface Methodology (RSM)

RSM is an experimental strategy that explores the space of process independent variables and empirical statistical modeling to establish appropriate relationships between responses (outputs) and process variables or factors (inputs). In this study, in order to correlate process parameters and wear rates, empirical relationships were established to predict responses based on experimental measurements. The response is a function of the volume % (P) of porosity present in the coating, the velocity of the eroded particles (V), the angle of impact of the eroded particles (A) and the flux of the eroded particles (F), which can be expressed as

$$\text{Responses} = \{f(P, V, A, F)\}$$

The empirical relationship chosen includes the main influences and interactions of all factors. The process of constructing empirical relationships and calculating regression coefficient values can be mentioned elsewhere.

3.3. Microhardness measurement

The microhardness distribution is a function of the distance from the coating-substrate interface. The average microhardness of the coating and substrate were 428 ± 48 and 189 ± 10 HV, respectively. The significant increase in microhardness at the interface is due to the work hardening of the substrate during the blasting process caused by shot peening. Due to the uniformity of the coating structure, the microhardness of the coating was observed to vary along the cross section.

3.4. Effect of erodent particle impact angle on erosion rate

The effect of the impact angle on the erosion rate of the coating is shown. The mechanism by which material is removed from the surface during erosion, erosion can be ductile or brittle. The typical feature of the ductile process is the greatest waste at low impact angles. Most metallic materials are eroded by this mechanism. On the other hand, for brittle materials, the erosion process is characterized by a maximum waste at high impact angles at which erosion occurs by cracking and chipping of the surface material.

3.5. Erosion under low erodent particle impact angles

The worn surface of the ceramic coating eroded at an impact angle of 30° exhibits severe plastic shear deformation caused by the sliding action of the erosive particles. There is evidence that the impact particles have friction, extrusion, ploughing and cutting. There is also evidence of brittle cracking that eventually leads to material fragmentation. In the photomicrograph, one can see plastic shear and friction bands, which are produced by corroding particles that rub against the surface during the etching process. An etch pit is formed by the crack, which can be seen in the photomicrograph. Since the contact of the erosive particles with the target surface at a shallow impact angle of 30° is mainly due to ploughing and is very susceptible to embrittlement cracking, the erosion at this impact angle is very low.

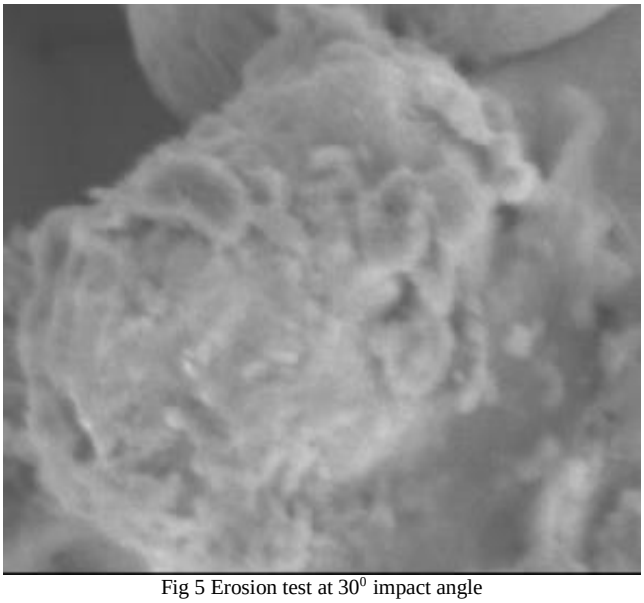

Fig 5 Erosion test at 30^0 impact angle

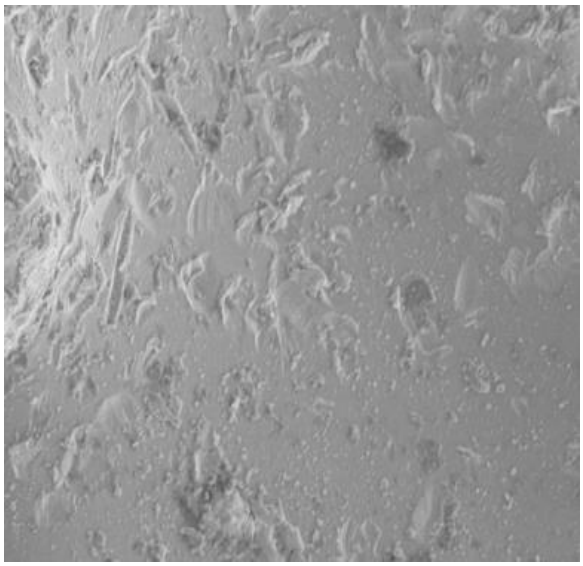

Fig.6 Erosion test at 90^0 impact angle

3.6 Effect of coating porosity on erosion rate

Erosion is generally considered to be a number of quasi-static single impacts. If there is a pre-existing defect, lateral cracking will occur at a low energy threshold. As expected, the erosion rate increases as the volume percentage of porosity increases. Plasma-sprayed ceramic coatings fail through the propagation of cracks around crack boundaries and micro-crack networks, which are inherent to the microstructure of plasma sprayed ceramic coatings and provide some degree of strain tolerance under thermal cycling conditions. This is not the case with plasma sprayed ceramic coatings under solid particle erosion. When polished and then eroded, it quickly returns to a surface finish similar to the spray value, if not bad. For the erosion mechanism based on residual tensile stress, the porosity at which cracking occurs is hardly increased with respect to a large amount of uniform plastic deformation at the time of fracture. The effect of porosity on material erosion behaviour depends on their microstructure and erosion conditions. For ceramic coatings with different porosity percentages, three different types of erosion mechanisms and associated erosion rates have been observed in current research.

4. CONCLUSION

In this study, considering the effect of solid particle erosion in the two parameters, the volume % of porosity present in the coating is the most important factor affecting the rate of coating erosion. The factors (parameters), ie the impact velocity of the corroded particles, the impact angle of the corroded particles and the flux, can be considered separately as the next most important parameter affecting the erosion rate.

It should be emphasized that the range, results and conclusions selected for the parameters relate specifically to the air jet erosion test apparatus used in this study. However, the methods shown and methods of responding to surfaces are common.

REFERENCES:

[1] Mathapati, M., Ramesh, M. R., & Doddamani, M. (2017). Surface & Coatings Technology High temperature erosion behavior of plasma sprayed NiCrAlY / WC-Co / cenosphere coating, *325*, 98–106.

[2] Ramachandran, C. S., Balasubramanian, V., & Ananthapadmanabhan, P. V. (2013). Erosion of atmospheric plasma sprayed rare earth oxide coatings under air suspended corundum particles. *Ceramics International*, *39*(1), 649–672. https://doi.org/10.1016/j.ceramint.2012.06.077

[3] Sharma, S. (2012). High Temperature Erosive Wear Study of NiCrFeSiB Flame Sprayed Coatings, *93*(September), 7–12. https://doi.org/10.1007/s40033-012-0006-9

[4] Xia, Z., Zhang, X., & Song, J. (1999). Erosion-Resistance of Plasma Sprayed Coatings, *8*(December), 716–718.

[5] Yang, Q., & Mckellar, R. (2015). Tribology International Nanolayered CrAlTiN and multilayered CrAlTiN – AlTiN coatings for solid particle erosion protection. *Tribiology International*, *83*, 12–20. https://doi.org/10.1016/j.triboint.2014.11.002